



## PHOTOCATALYTIC DEGRADATION OF ERYTHROSIN-B IN THE PRESENCE OF TIN DIOXIDE

SHIKHA PANCHAL<sup>\*</sup>, YUVRAJ JHALA<sup>a</sup>, ANURADHA SONI<sup>a</sup> and RITU VYAS<sup>b</sup>

Deptt. of Chemistry, Pacific College of Basic & Applied Sciences, PAHER University, UDAIPUR – 313003 (Raj.) INDIA

<sup>a</sup>Deptt. of Chemistry, B. N. P.G. College, UDAIPUR – 313002 (Raj.) INDIA

<sup>b</sup>Deptt. of Chemistry, Pacific Institute of Technology, UDAIPUR – 313003 (Raj.) INDIA

(Received : 27.12.2013; Accepted : 09.01.2014)

### ABSTRACT

In the present study, the photocatalytic degradation of Erythrosine-B was studied in presence of semiconductor tin dioxide. The progress of the reaction was observed spectrophotometrically at 520 nm. The effect of various operating variables like pH, concentration of dye, amount of semiconductor and light intensity on the rate of degradation was observed. A tentative mechanism has also been proposed for the photocatalytic degradation of dye.

**Key words:** Photocatalytic, Degradation, Erythrosine-B, Tin dioxide.

### INTRODUCTION

Water pollution is one of the world's greatest problems of today. The domestic use and industrial activity especially in developed countries produced large amount of wastewater. The release of dyes into the environment constitutes a large proportion of water pollution. The coloured wastewaters represent a serious environmental problem and a public health concern. Several methods have been used for the removal of dyes from the environment, including physical, chemical and biological processes, but each one has its own advantages and limitations. Photocatalytic treatment methods are favored as they are considered eco-friendly and relatively low cost for the degradation of these pollutants.

Since the last three decades, heterogeneous photocatalytic oxidation process has been studied extensively for the destructive oxidation of various organic pollutants. Kako et al.<sup>1</sup> investigated prevention against H<sub>2</sub>S-derived catalyst deactivation on Pd catalyst (Pd/TiO<sub>2</sub>) using TiO<sub>2</sub> photocatalytic reaction. Katsoni et al.<sup>2</sup> investigated advanced oxidation processes to degrade trinitrophenol in model aqueous solutions by catalytic wet air oxidation and solar TiO<sub>2</sub> photocatalysis. Enesca et al.<sup>3</sup> prepared six SnO<sub>2</sub>-TiO<sub>2</sub> tandem semiconductor samples by spray pyrolysis deposition using different precursor compositions and deposition temperatures. Torres-Martínez et al.<sup>4</sup> reported the efficient photocatalytic degradation of *p*-nitrophenol and Acid orange 7 using ZnS nanocrystals (~ 3 to 5 nm diameter) produced in gram quantities with > 50% product yield.

Cheng and Kang<sup>5</sup> prepared Bi<sub>2</sub>O<sub>3</sub> visible light responsive photocatalysts by chemical precipitation and consequent calcination process. The photocatalyst had strong absorption for visible light and efficient separation of charge carrier, which made it a good photocatalyst towards degradation of Malachite green. A

facile solvothermal–calcining route for the large-scale synthesis of uniform  $\beta$ - $\text{Bi}_2\text{O}_3$  nanospheres has been demonstrated by Xiao et al.<sup>6</sup> Adhikari et al.<sup>7</sup> used  $\text{Er}^{3+}/\text{Yb}^{3+}$  co-doped  $\text{Bi}_2\text{MoO}_6$  photocatalyst for the decomposition of Rhodamine B under simulated solar light irradiation. Semiconductor iron (III) oxide was used in photocatalytic bleaching of some dyes by Ameta et al.<sup>8</sup> Hidalgo et al.<sup>9</sup> prepared local zirconium and iron arrangements of the iron-doped  $\text{ZrO}_2$ - $\text{TiO}_2$  system, by sol–gel impregnation method. The photocatalytic activity of the undoped and iron-doped binary system  $\text{ZrO}_2$ - $\text{TiO}_2$  was investigated in two kind of photoreactions: the salicylic acid photooxidation and the photocatalytic reduction of Cr (VI). A new composite photocatalyst ( $\text{Fe}_2\text{O}_3$  and  $\text{ZrO}_2/\text{Al}_2\text{O}_3$ ) combining the properties of both semiconductor and Fenton like catalyst was prepared by Liu et al.<sup>10</sup>

Stodolny and Laniecki<sup>11</sup> prepared two series of  $\text{Ta}_2\text{O}_5$ - $\text{TiO}_2$  photocatalysts (Ta: Ti = 4:1, 1:1 and 1:4) by sol–gel technique applying triblock copolymer of Pluronic P123 and tested it in platinized form (0.3 wt.%) for photodecomposition of water under ultraviolet and visible light ( $\lambda > 300$  nm). The mixed oxides of  $\text{Ta}_2\text{O}_5$ - $\text{TiO}_2$  system showed much lower band-gap than pure  $\text{Ta}_2\text{O}_5$  and relatively high activity in platinized state in photocatalytic hydrogen generation under visible light. Yang et al.<sup>12</sup> synthesized  $\text{SnO}_2/\text{ZnO}/\text{TiO}_2$  composite photocatalysts. They also tested its photocatalytic activity with photodecomposition of Methyl orange under both; visible and UV light irradiations. Kuzhalosai et al.<sup>13</sup> reported that  $\text{SnO}_2$  loaded ZnO ( $\text{SnO}_2$ -ZnO) was more efficient for the degradation of Acid orange 10 than commercial ZnO, bare ZnO,  $\text{TiO}_2$ -P25 and  $\text{TiO}_2$  (Merck).

The photocatalytic behavior of the  $\text{SnO}_2/\text{V}_2\text{O}_5$  nanowires for the photodegradation of Toluidine blue O dye under UV exposure was examined by Shahid et al.<sup>14</sup> Erkan et al.<sup>15</sup> reported the photocatalytic antimicrobial activity over  $\text{TiO}_2$ ,  $\text{SnO}_2$  and their Pd doped thin film samples against *Escherichia coli*, *Staphylococcus aureus*, *Saccharomyces cerevisiae* and *Aspergillus niger* spores.  $\text{SnO}_2$  was found to show lower photocatalytic efficiency against *E. coli* with a 56% decrease in survival after 2 h illumination and a 68% decrease in survival of *E. coli* after palladium addition.

## EXPERIMENTAL

A stock solution of Erythrosine B ( $1.0 \times 10^{-3}$  M) was prepared in doubly distilled water. This stock solution was further diluted as and when required. The optical density of Erythrosine B solution was determined with the help of spectrophotometer at  $\lambda_{\text{max}} = 520$  nm. The dye solution was divided into four parts and control experiments were performed.

- The first beaker containing Erythrosine-B solution was kept in the dark.
- The second beaker containing Erythrosine-B was exposed to a 200 W tungsten lamp.
- The third beaker containing Erythrosine-B solution and 0.10 g tin dioxide was kept in dark.
- The fourth beaker containing Erythrosine-B solution and 0.10 g tin dioxide was exposed to a 200 W tungsten lamp.

After keeping these beakers for a few hours, the optical density of the solution in each beaker was measured with the help of a spectrophotometer. It was found that the solutions of the first three beakers had almost the same optical density as their initial value while it decreases in the solution of the fourth beaker. From this observation, it becomes clear that this reaction required the presence of both; light and the semiconductor tin dioxide. Hence, this reaction is photocatalytic in nature.

$1.0 \times 10^{-5}$  M solution of Erythrosine B was prepared in doubly distilled water and 0.10 g of tin dioxide was added to it. The pH of the reaction mixture was kept to 8.5 and this solution was exposed to a

200 W tungsten lamp. A decrease in optical density of Erythrosine B solution was observed with increasing time of exposure. The typical run for the photocatalytic degradation of Erythrosine B in the presence of SnO<sub>2</sub> photocatalyst has been presented in Table 1 and graphically represented in Fig. 1

**Table 1: A typical run**

Time (min.)	Absorbance (A)	1 + log A
0.0	0.812	0.9096
10.0	0.768	0.8954
20.0	0.759	0.8802
30.0	0.737	0.8675
40.0	0.715	0.8543
50.0	0.685	0.8357
60.0	0.660	0.8195
70.0	0.644	0.8089
80.0	0.621	0.7931
90.0	0.593	0.7731
100.0	0.587	0.7686
110.0	0.557	0.7459
120.0	0.530	0.7243
130.0	0.519	0.7152
140.0	0.500	0.6990
150.0	0.480	0.6812
160.0	0.462	0.6646

Rate constant (k) =  $5.83 \times 10^{-5} \text{ sec}^{-1}$

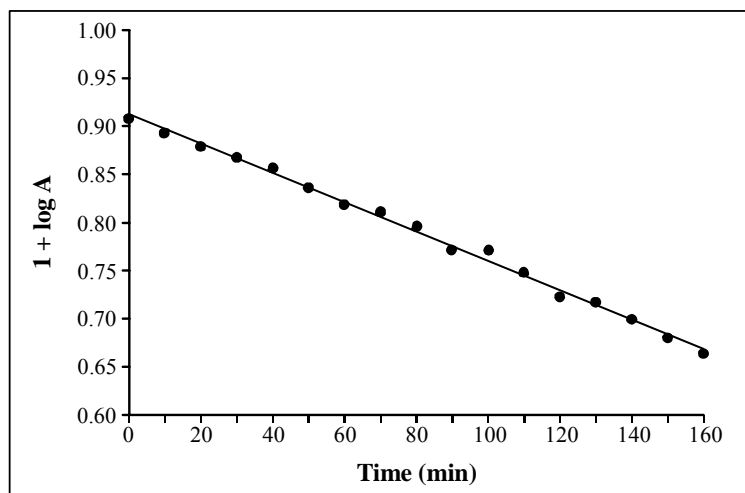


**Fig 1: A typical run**

The plot of  $1 + \log A$  v/s time was linear and hence, it has been concluded that this reaction follows pseudo-first order kinetics. The rate of this reaction was determined by the expression (1)

$$k = 2.303 \times \text{slope} \quad \dots(1)$$

### Effect of pH

The effect of pH on the rate of degradation of dye solution was investigated in the pH range (4-9.5). The results are reported in Table 2 and graphically presented in Fig. 2

**Table 2: Effect of pH**

[Erythrosine B] =  $1.0 \times 10^{-5}$  M

SnO<sub>2</sub> = 0.10 g

Light intensity = 50.0 mWcm<sup>-2</sup>

pH	Rate constant (k) × 10 <sup>5</sup> (sec <sup>-1</sup> )
4.0	5.11
5.0	5.16
6.0	5.24
7.0	5.36
8.0	5.40
<b>8.5</b>	<b>5.83</b>
9.0	5.00
9.5	4.89

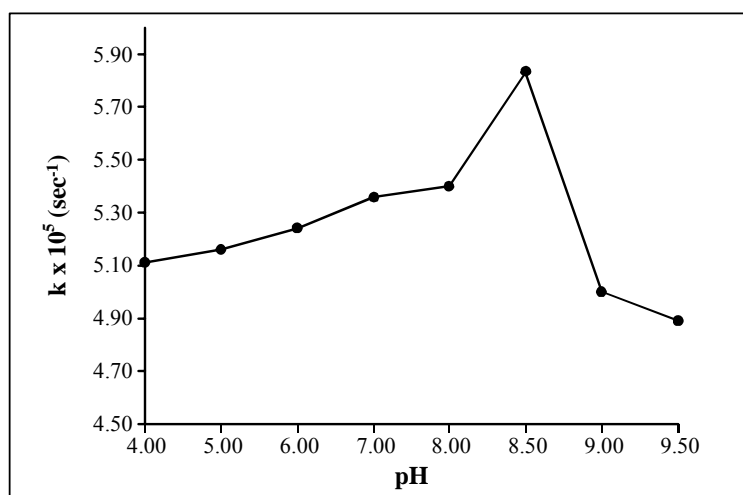


**Fig. 2: Effect of pH**

It has been observed that the rate of degradation was increased with increase in pH from 4.0 to 8.5; further increase in pH results in a decrease in the rate of reaction. The increase in the rate of photocatalytic degradation with increase in pH may be due to generation of more  $\cdot\text{OH}$  radicals, which are produced from the interaction of  $\text{OH}^-$  and hole ( $h^+$ ) of the semiconductor. These  $\cdot\text{OH}$  radicals are responsible for the oxidative degradation of dye. After pH 8.5, the rate decreases because more  $\text{OH}^-$  ions are available and these

will be adsorbed on the surface of the semiconductor making it negatively charged so that the approach of anionic Erythrosine B to the semiconductor surface will be retarded due to repulsion between two negatively charged species. This will result into decrease in the rate of degradation.

### Effect of Erythrosine B concentration

The effect of dye concentration on the rate of degradation of Erythrosine B was investigated. The results are reported in Table 3 and graphically presented in Fig. 3.

**Table 3: Effect of Erythrosine B concentration**

pH = 8.5

Light intensity = 50.0 mW cm<sup>-2</sup>

SnO<sub>2</sub> = 0.10 g

[Erythrosine B] × 10 <sup>5</sup> M	Rate constant (k) × 10 <sup>5</sup> (sec <sup>-1</sup> )
0.4	3.05
0.6	5.29
0.7	5.50
0.8	5.74
0.9	5.79
<b>1.0</b>	<b>5.83</b>
1.1	5.24
1.2	4.61
1.3	4.50
1.4	4.40

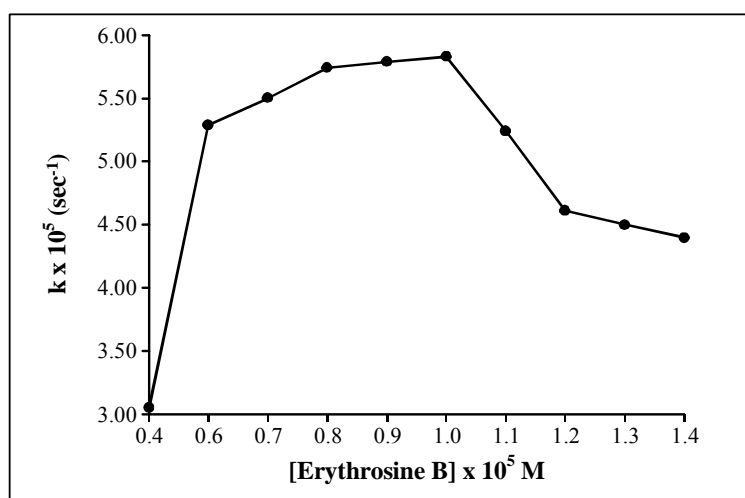


**Fig. 3: Effect of dye concentration**

It has been observed that the rate of photocatalytic degradation increases with increase in concentration of dye up to  $1.0 \times 10^{-5}$  M. The rate of photocatalytic degradation was found to decrease with an increase in the concentration of dye further. This may be attributed to the fact that as the concentration of

dye was increased, more dye molecules were available for excitation followed by inter system crossing and hence, there was an increase in the rate. The rate of photocatalytic degradation was found to decrease with an increase in the concentration of dye further. Here, the dye starts acting as a filter for the incident light and it does not permit the desired light intensity to reach the semiconducting particles and thus, decreasing the rate of the photocatalytic bleaching of dye.

### Effect of amount of photocatalyst

The rate of degradation of dye was also affected by the amount of semiconductor and therefore different amounts of semiconductor were used. The results are reported in Table 4 and graphically presented in Fig. 4.

**Table 4: Effect of amount of photocatalyst**

pH = 8.5

Light intensity = 50.0 mW cm<sup>-2</sup>

[Erythrosine B] = 1.0 × 10<sup>-5</sup> M

SnO <sub>2</sub> (g)	Rate constant (k) × 10 <sup>5</sup> (sec <sup>-1</sup> )
0.02	4.35
0.04	5.24
0.06	5.46
0.08	5.53
<b>0.10</b>	<b>5.83</b>
0.12	5.80
0.14	5.82

Here the data indicate that as the amount of photocatalyst was increased, the rate of degradation also increases but after the amount 0.10 g of photocatalyst, it shows saturation like behaviour. It may be due to fact that the as the amount of semiconductor was increased, the exposed surface area of the semiconductor also increased. After this, the rate of degradation decreases, as the catalyst amount was increased. Because it only increases the thickness of the layer of semiconductor, and not the exposed surface area.

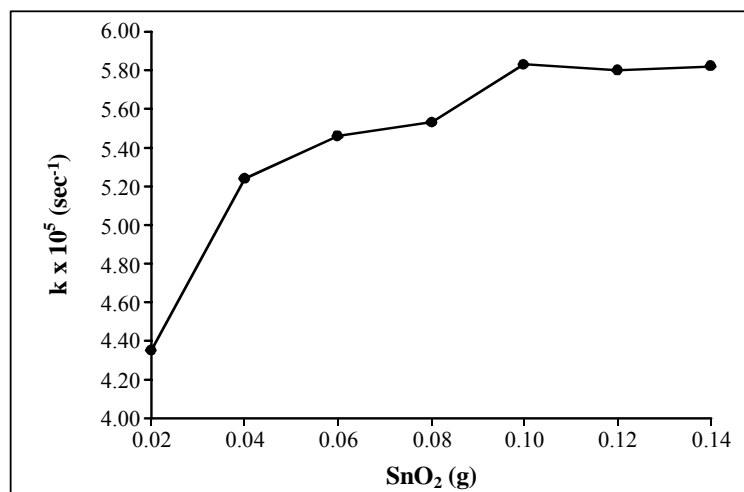


**Fig. 4: Effect of amount of photocatalyst**

### Effect of light intensity

The effect of light intensity on the photocatalytic degradation of the dye was investigated. It was observed that degradation of dye was enhanced on increasing the intensity of light. The results are reported in Table 5 and graphically presented in Figure 5

**Table 5: Effect of light intensity**

pH = 8.5 SnO<sub>2</sub> = 0.10 g  
 [Erythrosine B] = 1.0 × 10<sup>-5</sup> M

Light intensity (mW cm <sup>-2</sup> )	Rate constant (k) × 10 <sup>5</sup> (sec <sup>-1</sup> )
10.0	3.13
20.0	3.74
30.0	4.51
40.0	5.11
<b>50.0</b>	<b>5.83</b>
60.0	7.01

An almost linear relationship between light intensity and the rate of reaction was observed. It was observed that degradation of dye was enhanced on increasing the intensity of light. This may be due to an increase in the number of photon striking per unit time, per unit area of tin dioxide powder on increasing the intensity of light. However, higher intensities were avoided due to thermal effects.

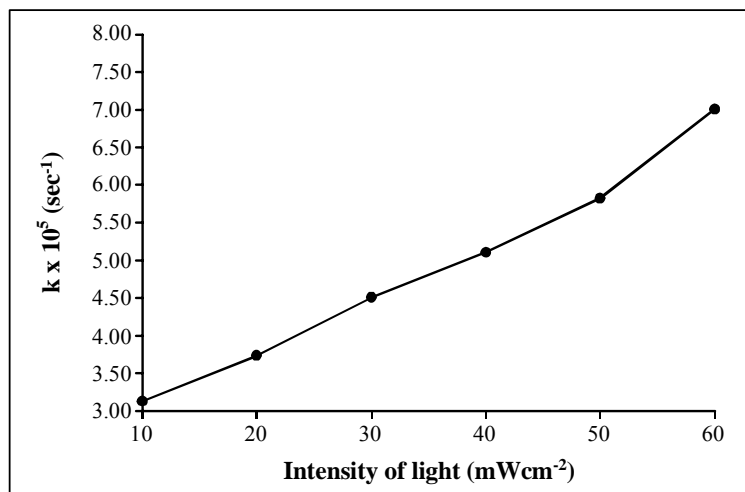


**Fig 5: Effect of light intensity**

### Effect of doping

The typical run for the photocatalytic degradation of Erythrosine B in the presence of iron doped SnO<sub>2</sub> photocatalyst has been presented in Table 6 and graphically represented in Fig. 6. It was observed that the rate of degradation of Erythrosine B increases from 5.83 × 10<sup>-5</sup> to 7.18 × 10<sup>-5</sup> sec<sup>-1</sup> on iron doped tin dioxide. It gives about 23.15% rise in the rate, which means that iron doping enhances the photocatalytic activity of tin dioxide.

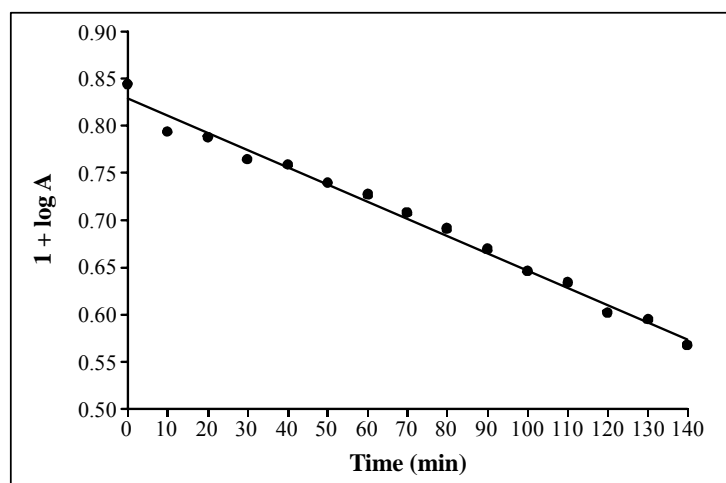
**Table 6: A typical run**

pH = 8.5  
[Erythrosine B] =  $1.0 \times 10^{-5}$  M

Fe doped SnO<sub>2</sub> = 0.10 g  
Light intensity = 50.0 mW cm<sup>-2</sup>

Time (min.)	Absorbance (A)	1 + log A
0.0	0.700	0.8451
10.0	0.622	0.7938
20.0	0.615	0.7889
30.0	0.582	0.7649
40.0	0.572	0.7574
50.0	0.549	0.7396
60.0	0.531	0.7251
70.0	0.508	0.7059
80.0	0.488	0.6884
90.0	0.465	0.6675
100.0	0.442	0.6454
110.0	0.428	0.6314
120.0	0.401	0.6031
130.0	0.392	0.5933
140.0	0.371	0.5694

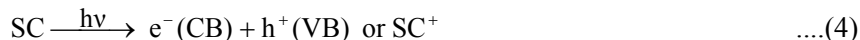
Rate constant (k) =  $7.18 \times 10^{-5}$  sec<sup>-1</sup>

**Fig. 6: A typical run****Mechanism**

On the basis of the experimental observations a tentative mechanism of photocatalytic degradation of Erythrosine B may be proposed as-

Erythrosine B (EB) absorbs radiation of suitable wavelength and it is excited to its first singlet state followed by intersystem crossing (ISC) to triplet state. On the other hand, the semiconducting tin dioxide

also utilizes the incident light energy to excite its electron from valence band to conduction band; thus, leaving behind a hole. This hole may abstract an electron from hydroxyl ions to generate hydroxyl radicals. These hydroxyl radicals will then oxidize the dye to its leuco form, which may ultimately degrade to products.



The participation of  $\cdot\text{OH}$  radicals as an active oxidizing species was confirmed by using hydroxyl radical scavengers (isopropanol), where the rate of degradation was drastically reduced.

## REFERENCES

1. T. Kako, H. Irie and K. Hashimoto, Prevention against Catalytic Poisoning by  $\text{H}_2\text{S}$  utilizing  $\text{TiO}_2$  Photocatalyst, *J. Photochem. Photobiol. A*, **171**, 131-135 (2005).
2. A. Katsoni, H. T. Gomes, L. M. Pastrana-Martínez, J. L. Faria, J. L. Figueiredo, D. Mantzavinos and A. M. T. Silva, Degradation of Trinitrophenol by Sequential Catalytic Wet Air Oxidation and Solar  $\text{TiO}_2$  Photocatalysis, **172**, 634-640 (2011).
3. A. Enesca, L. Isac, L. Andronic, D. Perniu and A. Duta, Tuning  $\text{SnO}_2$ - $\text{TiO}_2$  Tandem Systems for Dyes Mineralization, *Appl. Catal., B*, **147**, 175-184 (2014).
4. C. L. Torres-Martínez, R. Kho, O. I. Mian and R. K. Mehra, Efficient Photocatalytic Degradation of Environmental Pollutants with Mass-produced  $\text{ZnS}$  Nanocrystals, *J. Colloid Interface Sci.*, **240(2)**, 525-532 (2001).
5. L. Cheng and Y. Kang, Selective Preparation of  $\text{Bi}_2\text{O}_3$  Visible Light-driven Photocatalyst by Dispersant and Calcination, *J. Alloys Compd.*, **585**, 85-93 (2014).
6. X. Xiao, R. Hu, C. Liu, C. Xing, C. Qian, X. Zuo, J. Nan and L. Wang, Facile Large-Scale Synthesis of  $\beta$ - $\text{Bi}_2\text{O}_3$  Nanospheres as a Highly Efficient Photocatalyst for the Degradation of Acetaminophen under Visible Light Irradiation, *Appl. Catal.*, **140-141**, 433-443 (2013).
7. R. Adhikari, G. Gyawali, S. H. Cho, R. Narro-García, T. Sekino and S. W. Lee,  $\text{Er}^{3+}/\text{Yb}^{3+}$  Co-doped Bismuth Molybdate Nanosheets Upconversion Photocatalyst with Enhanced Photocatalytic Activity, *J. Solid State Chem.*, **209**, 74-81 (2014).
8. S. C. Ameta, R. Ameta, J. Vardia and P. B. Panjabi, *Int. J. Chem. Technol.*, **13(2)**, 114 (2006).
9. M. C. Hidalgo, G. Colón, J. A. Navio, M. Macias, V. V. Kriventsov, D. I. Kochubey, M. V. Tsodikov, EXAFS Study and Photocatalytic Properties of Un-Doped and Iron-Doped  $\text{ZrO}_2$ - $\text{TiO}_2$  (Photo-) Catalysts, *Catal. Today*, **128(3-4)**, 245-250 (2007).

10. W. Liu, F. Zeng, H. Jiang, X. Zhang and W. Li, Composite Fe<sub>2</sub>O<sub>3</sub> and ZrO<sub>2</sub>/Al<sub>2</sub>O<sub>3</sub> Photocatalyst: Preparation, Characterization, and Studies on the Photocatalytic Activity and Chemical Stability, *Chem. Eng. J.*, **180**, 9-18 (2012).
11. M. Stodolny and M. Laniecki, Synthesis and Characterization of Mesoporous Ta<sub>2</sub>O<sub>5</sub>-TiO<sub>2</sub> Photocatalysts for Water Splitting, *Catal. Today*, **142(3-4)**, 314-319 (2009).
12. G. Yang, Z. Yan and T. Xiao, Preparation and Characterization of SnO<sub>2</sub>/ZnO/TiO<sub>2</sub> Composite Semiconductor with Enhanced Photocatalytic Activity, *Appl. Surf. Sci.*, **258(22)**, 8704-8712 (2012).
13. V. Kuzhalosai, B. Subash, A. Senthilraja, P. Dhatshanamurthi and M. Shanthi, Synthesis, Characterization and Photocatalytic Properties of SnO<sub>2</sub>-ZnO Composite under UV-A Light, *Spectrochim. Acta, Part A*, **115**, 876-882 (2013).
14. M. Shahid, I. Shakir, S. Yang and D. J. Kang, Facile Synthesis of Core-Shell SnO<sub>2</sub>/V<sub>2</sub>O<sub>5</sub> Nanowires and their Efficient Photocatalytic Property, *Mater. Chem. Phys.*, **124(1)**, 619-622 (2010).
15. A. Erkan, U. Bakir and G. Karakas, Photocatalytic Microbial Inactivation over Pd Doped SnO<sub>2</sub> and TiO<sub>2</sub> Thin Films, *J. Photochem. Photobiol. A*, **184(3)**, 313-321 (2006).